Journal of Solid State Chemistry 231 (2015) 159–162

Contents lists available at ScienceDirect

Journal of Solid State Chemistry

journal homepage: www.elsevier.com/locate/jssc

Heavy ion irradiation-induced microstructural evolution in pyrochlore $Lu_2Ti_2O_7$ at room temperature and 723 K

Q.R. Xie, J. Zhang *, X.N. Dong, Q.X. Guo, N. Li

College of Energy, Xiamen University, Xiamen, Fujian 361005, China

ARTICLE INFO

Article history:
Received 29 April 2015
Received in revised form
7 July 2015
Accepted 4 August 2015
Available online 5 August 2015

Keywords:
Phase transformation
Nano-crystal
Ion irradiation

ABSTRACT

Polycrystalline pyrochlore $Lu_2Ti_2O_7$ pellets were irradiated with 600 keV Kr^{3+} at room temperature and 723 K to a fluence of 4×10^{15} ions/cm^2, corresponding to an average ballistic damage dose of 10 displacements per atom in the peak damage region. Irradiation-induced microstructural evolution was examined by grazing incidence X-ray diffraction, and cross-sectional transmission electron microscopy. Incomplete amorphization was observed in the sample irradiated at room temperature due to the formation of nano-crystal which has the identical structure of pyrochlore, and the formation of nano-crystal is attributed to the mechanism of epitaxial recrystallization. However, an ordered pyrochlore phase to a swelling disordered fluorite phase transformation is occurred for the $Lu_2Ti_2O_7$ sample irradiated at 723 K, which is due to the disordering of metal cations and anion vacancies.

1. Introduction

Pyrochlore (belongs to a space group , no. 227, in International Tables for Crystallography) is a superstructure of the fluorite (MO_2), except that there are two cation sites and one-eighth of missing anions [1]. The pyrochlore compounds with composition have attracted more attention in recent years [2]. The large A^{3+} cation is at 16d site, eight-coordinated and located within a distorted cubic coordination polyhedron, while the smaller B^{4+} cation is at 16 c site, six-coordinated and located within a distorted octahedron [3]. The (3+,4+) pyrochlores are of interest in nuclear waste management because of their ability to incorporate trivalent lanthanides and tri- and tetravalent actinides.

Incorporation of actinides into ceramics is an important issue for the immobilization of actinide-bearing waste streams. Pyrochlore is a potential candidate for the immobilization of high level waste (HLW) and dismantled plutonium due to their wide incorporation ability for actinides and rare earth elements [4–6]. On the other hand, the naturally occurring pyrochlores are often found to be metamict (aperiodic) as a result of radiation damage from uranium and thorium transmutation [7]. An important aspect of assessing the physical and chemical durability of pyrochlore as a nuclear waste form is to understand atomic-scale changes caused by α-decay event damage [8,9]. Irradiation damage, especially amorphization, generally decreases the chemical durability of nuclear waste form in the repository environment because of the lower thermodynamic stability and higher impregnation rate of the irradiation damaged materials. During the past two decades, heavy ion irradiation experiments, substituting for short half-life actinide-doping (such as ^{244}Cm), were used to simulate α-decay event in waste form, due to its ease of handling the irradiation samples over a much shorter period of time. The radiation susceptibility of nuclear form pyrochlore-$Lu_2Ti_2O_7$ had been examinaed, and previous liquid nitrogen (LN2, 77 K) irradiation and in-situ TEM studies demonstrated that the pyrochlore ceramic can become fully amorphous under 1 dpa [3,10]. However, the pyrochlore-$Lu_2Ti_2O_7$ can not become completed amorphous in our bulk sample irradiated at room temperature, even under a peak dpa of ~10 because of the nano-crystals formation. Furthermore, previous studies pay their attention to the radiation effects below critical temperature, while few irradiation-induced evolutions of pyrochlore-$A_2Ti_2O_7$ above critical temperature are reported. In this study, the pyrochlore $Lu_2Ti_2O_7$ samples, which have the lowest critical temperature T_c=473 K in pyrochlore-$A_2Ti_2O_7$ [3], were irradiated with 600 keV Kr^{3+} ions to a fluence of 4×10^{15} ions/cm^2 at RT and 723 K. The grazing incidence X-ray diffraction (GIXRD), and ex-situ TEM were implemented to determine the microstructural evolution induced by Krypton ion irradiation under (RT) and above critical temperature (723 K) in bulk samples.

2. Experimental

Polycrystalline pyrochlore $Lu_2Ti_2O_7$ pellets were prepared by traditional ceramic processing. The Lu_2O_3 (99.99% pure) and TiO_2 (99.99% pure) powers were first heated at 1000 °C for 10 h to

* Corresponding author.
E-mail addresses: zhangjian@xmu.edu.cn, jianchng@gmail.com (J. Zhang).

http://dx.doi.org/10.1016/j.jssc.2015.08.005
0022-4596/

remove moisture and other volatile impurities. Stoichiometric amounts of the reactants were weighed to acquire the composition of $Lu_2Ti_2O_7$. Firstly, the thoroughly ground mixtures were heated in the pellet form at 1300 °C for 24 h. In order to attain a better homogeneity, the products obtained after first heating were reground, pelletized, and sintered at 1450 °C for 48 h. Then, pellets were cut with a diamond saw, and the specimens were polished to a 0.5 μm diamond finish. These pellets were examined with normal X-ray Diffraction, and found possess the pyrochlore structures. The measured density of these samples was found to be 7.038 g/cm^3, approximately 96% of their theoretical value (g/cm^3).

The well-polished samples were irradiated with 600 keV Kr^{3+} ions at room temperature (RT) and 723 K in the Ion Beam Materials Laboratory at Los Alamos National Lab, using a 200 kV Danfysik High Current Research Ion Implanter. The irradiation fluence is 4.0×10^{15} Kr^{3+}/cm^2. The 600 keV Kr^{3+} ions were implanted at normal incidence with an average flux of $\sim1.0\times10^{12}$ Kr/cm^2/s. The displacement damage and projectile depth profile of 600 keV Kr^{3+} ions in pyrochlore $Lu_2Ti_2O_7$ were estimated using the Monte Carlo program SRIM [11], where the threshold displacement energies of 40 eV were arbitrarily assumed for all atoms in the oxide ceramic. The simulated displacements per atom (dpa) and Kr ion concentration for the fluence of 4.0×10^{15} Kr^{3+}/cm^2 are shown in Fig. 1. The irradiation peak damage range, R_p, was estimated to be approximately 120 nm with a longitudinal straggling, ΔR_d, of ~60 nm.

Pristine and irradiated samples were characterized using grazing incidence X-ray diffraction (GIXRD). GIXRD measurements were performed using a Rigaku Ultima IV Advanced X-ray diffractometer, with Cu Kα radiation, $\alpha-2\theta$ geometry, parallel beams. The $\alpha-2\theta$ scans were performed using a step size of 0.02° and a dwell time of two seconds. X-ray patterns were recorded at a fixed glancing incidence angle of $\alpha=0.5°$ to investigate only the irradiation layer, and the implanted ion chemical effects can be ignored at the fluence of 4.0×10^{15} Kr^{3+}/cm^2 (Kr concentration is still less than 0.3 at% in the examined region). The penetration depth of X-ray is within 200 nm at incidence angle $\alpha=0.5°$ [12,13]. Integrated diffraction peak intensities were measured by fitting the diffraction patterns with pseudo-Voigt profiles to estimate the amorphization fraction. The cross-sectional TEM specimen was mechanically polished to a thickness below 10 μm using a diamond lapping film, followed by thinning to electron transparency using 4 keV Ar^+ ion milling. TEM observations of the sample irradiated at room temperature were performed using a Tecnai F30 instrument operating with an accelerating voltage of 300 kV, and the sample irradiated at 723 K were performed using a Tecnai G2 F20 S-Twin operating with an accelerating voltage of 200 kV. Selected area electron diffraction (SAED) patterns were used in this study to obtain electron diffraction patterns from small sample regions (diameter of ~150 nm).

3. Results and discussion

Fig. 2 shows the GIXRD patterns obtained from pristine $Lu_2Ti_2O_7$ and $Lu_2Ti_2O_7$ subjected to 600 keV Kr^{3+} ions to a fluence of 4.0×10^{15} Kr^{3+}/cm^2 at room temperature and 723 K. The incidence angle of X-ray is 0.5°, and the penetration depth of X-ray is estimated less than irradiation layer. The diffraction patters were normalized and offset for clarity. The diffraction patterns from the pristine sample are composed of principal diffraction maxima (labeled as $P_{(222)}$, $P_{(400)}$, $P_{(440)}$) and supperlattice reflections (labeled as $P_{(111)}$, $P_{(311)}$, $P_{(331)}$, $P_{(511)}$, $P_{(531)}$). After irradiation to fluence of 4.0×10^{15} Kr^{3+}/cm^2 at RT, all the diffraction patterns remain, while the diffraction peaks shift to smaller 2 angle, which is indicating a slightly swelling of lattice parameters. Moreover, an obvious diffusion halo shown up with a center at the $2\theta=32°$, which indicates an amorphous phase formed in the examination area. Therefore, the GIXRD observations imply that the sample irradiated at RT was partially amorphous with ~75% of amorphization in the basis of diffraction intensities calculation. As for irradiation at 723 K, the supper-lattice diffraction intensities diminish significantly. Besides, a set of diffraction patterns (marked with stars) are shown up on smaller 2θ side of pristine pyrochlore diffraction maxima, which can be indexed as (111), (200), and (220) plans of swelling defect fluorite phase. Therefore, a pyrochlore to a partial defect fluorite phase transformation was observed in the pyrochlore $Lu_2Ti_2O_7$ irradiated by 600 keV Kr^{3+} to a fluence of 4.0×10^{15} Kr^{3+}/cm^2 at 723 K.

Fig. 3 shows the cross-section TEM micrograph and corresponding SAED diffraction patterns of $Lu_2Ti_2O_7$ samples subjected to 600 keV Kr^{3+} ion irradiation to a fluence of 4×10^{15} ions/cm^2 at RT. The cross-section TEM image Fig. 3(a) demonstrates two distinctive diffraction contrasts due to the 600 keV Kr irradiation damage in pyrochlore $Lu_2Ti_2O_7$, and the thickness of damage layer is ~150 nm, in a reasonable agreement with the ion range of 600 keV Kr ions predicted by SRIM, $R_p+\Delta R_p$ (180 nm) shown in Fig.1. Furthermore, the SAED pattern Fig. 3(b) implies that nanosize crystals were formed in the damage layer, while Fig. 3

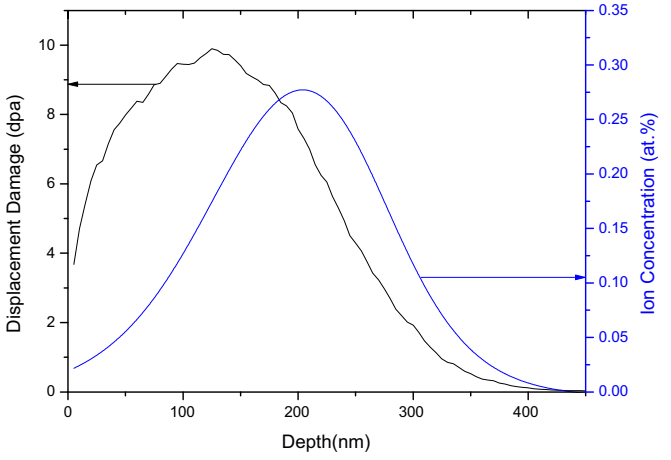

Fig. 1. SRIM simulation results of displacement damage and implanted Kr^{3+} ion concentration as a function of depth for 600 keV Kr^{3+} ion irradiation in $Lu_2Ti_2O_7$ to a fluence of 4.0×10^{15} ions/cm^2.

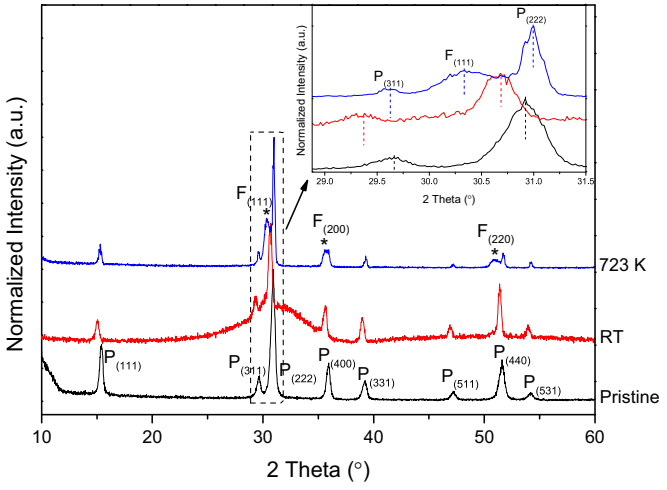

Fig. 2. GIXRD patterns of pristine $Lu_2Ti_2O_7$ pellets and $Lu_2Ti_2O_7$ irradiated by 600 keV Kr^{3+} to a fluence of 4.0×10^{15} ions/cm^2 at room temperature and 723 K (the incident angle of X-ray $\alpha=0.5°$).